IOPscience iopscience.iop.org

Home Search Collections Journals About Contact us My IOPscience

The effects of intervalley scattering on the cooling of hot carriers in $In_{0.53}Ga_{0.47}As$

This article has been downloaded from IOPscience. Please scroll down to see the full text article.

1994 J. Phys.: Condens. Matter 6 7589

(http://iopscience.iop.org/0953-8984/6/37/013)

View the table of contents for this issue, or go to the journal homepage for more

Download details:
IP Address: 171.66.16.151
The article was downloaded on 12/05/2010 at 20:32

Please note that terms and conditions apply.

J. Phys.: Condens. Matter 6 (1994) 7589–7601. Printed in the UK

The effects of intervalley scattering on the cooling of hot carriers in $In_{0.53}Ga_{0.47}As$

G R Hayes and R T Phillips
Cavendish Laboratory, Madingley Road, Cambridge CB3 0HE, UK

Received 21 April 1994

Abstract. The cooling of a hot electron–hole plasma in $In_{0.53}Ga_{0.47}As$ is studied by means of an analytical model. It is assumed that the carriers are thermalized at different effective temperatures and their distributions are of a Fermi–Dirac form from the shortest times. The energy-loss rates from the plasma due to coupling to transverse and longitudinal optical and acoustic phonon modes are included. Non-equilibrium phonon mode occupancy occurs, which decreases the cooling rate, but it proves necessary to incorporate $\Gamma \rightarrow L$ intervalley scattering into the model in order to provide a realistic description of recent experimental results. From this study we infer a $\Gamma \rightarrow L$ scattering time, at a lattice temperature of 4 K, of 500 ± 100 fs, and a return time of 9 ± 2 ps.

1. Introduction

The relaxation of electron–hole plasmas in direct-gap semiconductors, following intense laser excitation, has been extensively investigated over the last few years in the picosecond regime, and more recently in the sub-picosecond regime [1, 2], by time-resolved luminescence, and time-resolved Raman [3, 4] spectroscopy. These investigations initially concentrated on GaAs [1, 2] but have since been extended to InP [5, 6], CdTe [7], and various ternary alloys [8–11]. In conjunction with these experiments, analytical models based on Boltzmann's rate equations have been developed to explain the carrier cooling rates [7, 12–16]. Another theoretical approach involves Monte Carlo simulations which aim to explain the cooling rates without having to make any assumptions about the carrier distributions but these require a large number of computations to provide realistic results [17–19].

Experiments performed on $In_{0.53}Ga_{0.47}As$ have shown that the energy-loss rates of the hot carriers is up to two orders of magnitude smaller than predicted by simple theoretical models [9–11]. This has been attributed to a build-up of non-equilibrium LO phonons (the so-called 'hot-phonon effect') which can be re-absorbed by the hot carriers causing a retardation in the energy-loss rate. An analytical model which included the effect of phonon heating by calculating the phonon occupation number as a function of time was developed by Potz and Kocevar [13]. This model was subsequently used by Westland *et al* [10] to fit their experimental data. In these studies it was assumed that the electrons and holes instantaneously thermalized at the same carrier temperature. However, Asche and Sarbei's work [15] on the electron–hole (e–h) interaction showed that the holes remained at a far lower temperature than the electrons over the first few picoseconds after excitation, so any attempt to model the carrier cooling has to allow the electrons and holes to be thermalized at separate effective temperatures.

0953-8984/94/377589+13$19.50 © 1994 IOP Publishing Ltd

More recent work has concentrated on the importance of electron scattering to the L and X valleys [3, 20, 21]. This acts as an initial source of carrier cooling for the electrons as many high-energy electrons are removed from the Γ valley to the L valley where they no longer contribute to the luminescence. It then acts as a delayed source of heating as the electrons in the L valley migrate back to the Γ valley.

In this paper we reassess carrier cooling in $In_{0.53}Ga_{0.47}As$ in the light of new research, by presenting an analytical model which describes the cooling of the hot carriers and the build-up of a hot-phonon population. We show that it is necessary to allow the electrons and holes to be thermalized at different effective temperatures and also show that it is crucial to consider the effects of intervalley scattering when the laser energy is high enough to excite electrons above the threshold for transfer to the L valley. The approximations that are used simplify the models a great deal, but still provide sufficient accuracy to enable us to calculate the cooling of the electron–hole plasma down to a timescale of one picosecond which has not previously been possible in $In_{0.53}Ga_{0.47}As$. In the next section we present the theoretical models that we have used and in section 3 we compare the results of these models with the data measured by Gregory *et al* [22].

2. Theory

In this section we outline the models that are used to calculate the cooling curves of the photoexcited electrons in $In_{0.53}Ga_{0.47}As$. The first part involves a discussion of the main approximations that are used in these calculations. We will then describe the model relating to the cooling of a degenerate electron population in the single-spherical-valley approximation. Finally, we will discuss the effects of including multiple valleys in the carrier cooling calculations.

The primary assumption behind these models is that the energy input from the laser pulse instantaneously creates two thermalized carrier distributions, each with its own effective temperature, T_e and T_h, which is above the lattice temperature T_L. This approximation is justified because of the very rapid e–e and h–h interactions which broaden the initially sharp distribution over a wide energy range within the first 100 fs after excitation for the carrier densities that we are considering. The e–h scattering rate on the other hand, is much lower owing to the large difference between the effective masses of the two quasi-particles, so in general $T_e \neq T_h$ over the first few picoseconds. A recent experimental investigation [8] combined with an ensemble Monte Carlo calculation [19] confirmed the existence of separate effective electron and hole temperatures during the first 10 picoseconds in $Al_xGa_{1-x}As$.

The model for the valence band consists of a single spherical heavy-hole band. The light-hole band is neglected because its population will remain small compared with the heavy-hole population. In addition to this, light holes scatter less efficiently with the LO phonons than the heavy holes. However, as the mass of the light holes is much closer to that of the electron as compared to the heavy hole, their energy transfer rate due to electron–light-hole (e–lh) scattering will be much greater so this could act as a good energy-losses channel for the electrons. The effects of e–lh scattering will be examined at a later date. We will assume that the heavy-hole band is isotropic as the effects of anisotropy of the heavy-hole band is not noticeable after 0.1 ps [23]. Neglecting the non-parabolicity of the valence and conduction band may lead to a slight overestimation of the effective carrier temperature [21]. This error should be small however on the timescale that is considered here.

In this model, a static screening approximation is used to treat the carrier–LO phonon interaction and the interaction of carriers with LA phonons via the piezoelectric effect.

The validity of this approximation, however, has recently been questioned [24], so in section 3 the accuracy of the screening model will be briefly examined. Possible effects of screening of the acoustic deformation potential interaction are neglected here, as most of the energy loss of the carriers is via LO phonon emission. The carrier–TO phonon interaction is also unscreened because there are no macroscopic fields associated with TO phonons. We shall also treat the screening of the e–h interaction statically as this provides a very good approximation due to the pronounced mass difference [24].

We shall now consider the case of a single spherical valence band and a single conduction band. Following this, an improved model will be presented which includes satellite valleys in the conduction band and we will show how their inclusion is necessary to fit the experimental data on a picosecond timescale.

2.1. Single-valley model

To attempt to calculate the effective electron and hole temperatures as a function of time we start from the rate equations for the total energy of each carrier distribution, E_c (c = e, h) per unit volume

$$\left(\frac{dE_c}{dt}\right) = \left(\frac{dE_c}{dt}\right)_L + \left(\frac{dE_c}{dt}\right)_{ph} + \left(\frac{dE_c}{dt}\right)_{eh} + \left(\frac{dE_c}{dt}\right)_{rad} + \left(\frac{dE_c}{dt}\right)_{Aug} . \quad (1)$$

The first term in (1) corresponds to the power input to the carrier systems by the laser pulse which is assumed to be of 900 fs duration and have an energy of 1.44 eV per photon in order to model the data of Gregory *et al* [22]. The total carrier density created by the pulse is 1.9×10^{18} cm^{-3}. The amount of energy that is given to the electron (hole) by each absorbed photon can be determined by consideration of the conservation of energy and wave vector for two parabolic bands. The second term in (1) represents the rate of energy transfer between the carriers and the lattice due to the emission and absorption of phonons. This is given by

$$\left(\frac{dE_c}{dt}\right)_{ph} = -\sum_{j}^{\text{modes}} \sum_{i}^{\text{coupling}} \hbar\omega_{i,j} \left(\frac{dN_j(t)}{dt}\right)_i^c \quad (2)$$

where $\hbar\omega_{i,j}$ is the phonon energy and $N_j(t)$ is the phonon occupation number at time t. In our simulation we considered longitudinal optical (LO), acoustic (LA) and transverse optical (TO) and acoustic (TA) phonons. There were 1000 modes of each type extending from the zone centre to the zone boundary. LO and TO modes were assumed dispersionless and LA and TA modes of $|\sin(aq)|$ form with an amplitude fitted to the low-q sound velocities. This was a sufficient number to describe realistically the hot-phonon effect. Complications arising from the two-mode behaviour expected for the ternary system have been neglected. The rate of change of each phonon mode was calculated from Boltzmann's equation

$$\frac{dN_j(t)}{dt} = \sum_{c}^{\text{e,h}} \sum_{i}^{\text{coupling}} \left(\frac{dN_j(t)}{dt}\right)_i^c - \left(\frac{N_j(t) - N_j(0)}{\tau_j}\right). \quad (3)$$

Here, τ_j is the phonon decay time and takes account of anharmonic phonon decay. The value of τ_j in $In_{0.53}Ga_{0.47}As$ is uncertain at present so we use the value observed by Von der Linde *et al* [25] of 7 ps which was in GaAs at 77 K. This also agrees with the work of Kash *et al* [26] of 4.5–7 ps in GaAs at 20 K.

The rate of change of phonon mode occupancy due to the emission and absorption of phonons by the hot carriers is given by [27]

$$\left(\frac{\mathrm{d}N_j(t)}{\mathrm{d}t}\right)_i^{\mathrm{c}} = (N_j(t)+1)E_{i,j}^{\mathrm{c}} - N_j(t)A_{i,j}^{\mathrm{c}} \tag{4}$$

where

$$E_{i,j}^{\mathrm{c}} = \frac{m_{\mathrm{c}}^2 k_{\mathrm{B}} T_{\mathrm{c}}}{\pi\hbar^5} \frac{1}{\left(\exp\left(\frac{\hbar\omega_{i,j}}{k_{\mathrm{B}}T_{\mathrm{c}}}\right)-1\right)} \frac{B_{i,j}(q)}{q} \ln\left(\frac{1+\exp\left(\frac{\mu_{\mathrm{c}}}{k_{\mathrm{B}}T_{\mathrm{c}}} - \frac{1}{8m_{\mathrm{c}}k_{\mathrm{B}}T_{\mathrm{c}}}\left(\frac{2m_{\mathrm{c}}\omega_{i,j}}{q} - \hbar q\right)^2\right)}{1+\exp\left(\frac{\mu_{\mathrm{c}}}{k_{\mathrm{B}}T_{\mathrm{c}}} - \frac{1}{8m_{\mathrm{c}}k_{\mathrm{B}}T_{\mathrm{c}}}\left(\frac{2m_{\mathrm{c}}\omega_{i,j}}{q} + \hbar q\right)^2\right)}\right) \tag{5}$$

and

$$A_{i,j}^{\mathrm{c}} = E_{i,j}^{\mathrm{c}} \exp\left(\frac{\hbar\omega_{i,j}}{k_{\mathrm{B}}T_{\mathrm{c}}}\right). \tag{6}$$

Here, T_{c} and μ_{c} are the carrier temperatures and Fermi energies, q is the phonon wave vector, k_{B} is Boltzmann's constant and $m_{\mathrm{c=e,h}}$ is the effective mass of the electron or hole.

Electrons in the Γ valley coupled to LO phonons via the polar optical (PO) interaction whose coupling constant is given by [28]

$$B_{i,j}^{\mathrm{PO}}(q) = \frac{e^2\hbar\omega_{i,j}}{2\epsilon_0}\left(\frac{1}{K_\infty} - \frac{1}{K_0}\right)\frac{1}{q^2}\left(\frac{q^2}{q^2+q_{\mathrm{d}}^2}\right)^2. \tag{7}$$

They couple to LA modes through the acoustic deformation potential (DP)

$$B_{i,j}^{\mathrm{dp}}(q) = \frac{E_1^2\hbar q}{2\rho_{\mathrm{L}} s_1}. \tag{8}$$

They also couple to LA and TA modes via the piezoelectric effect (PZ). The coupling constant for this interaction is given by

$$B_{i,j}^{\mathrm{PZ}}(q) = \frac{e^2\hbar s_{1,t} K_{1,t}^2}{8\pi\epsilon_0 K_0}\frac{1}{q}\left(\frac{q^2}{q^2+q_{\mathrm{d}}^2}\right)^2 \cos^2\alpha. \tag{9}$$

Electrons do not couple to TO modes due to symmetry effects.

The holes also couple to all these modes. However, the coupling constants given in the previous equations must be reduced by a factor K, which is $\approx$ 2–2.5. This accounts for the reduced overlap due to the p-like nature of the holes in the valence band compared with the s-like wavefunctions of the electrons in the conduction band [29]. The holes also couple to TO modes through the optical deformation potential (ODP) as this is not forbidden by symmetry considerations in this case. Its coupling constant can be written as

$$B_{i,j}^{\mathrm{odp}}(q) = \frac{3d_0^2}{4\rho_{\mathrm{L}} s_1 a_0^2 q}. \tag{10}$$

Table 1. Material parameters for $In_{0.53}Ga_{0.47}As$ [37].

Definition	Symbol	Value
Energy gap	E_g	0.812 eV
Energy separation of L and Γ minima	E_L	0.55 eV
Electron effective mass	m_e	0.041 m_0
Hole effective mass	m_h	0.50 m_0
Static dielectric constant	K_0	13.73
Optical dielectric constant	K_∞	11.36
Lattice temperature	T_L	4 K
Mass density	ρ_L	5.59 g cm^{-3}
Lattice constant	a_0	5.87×10^{-10} m
LO phonon energy	$\hbar\omega_{LO,j}$	34.12 meV
TO phonon energy	$\hbar\omega_{TO,j}$	28.1 meV
Acoustic deformation potential	E_1	5.89 eV
Optical deformation potential	d_0	40 eV
Longitudinal peizoelectric constant	K_l	0.053
Transverse peizoelectric constant	K_t	0.053
Longitudinal sound velocity	s_l	4.81×10^5 m s^{-1}
Transverse sound velocity	s_t	3.5×10^5 m s^{-1}
Scattering angle	$\cos^2\alpha$	0.5
Overlap correction	K	2.5

The constants given in these equations are defined in table 1.

As previously discussed, screening of the e–ph and h–ph interactions is included in the simulation via the static screening approximation, i.e. by summing the time-dependent Thomas–Fermi susceptibilities of the separate carrier systems. The screening length is given by

$$q_d^2 = \frac{n_c e^2}{\epsilon_0 K_0 k_B}\left(\frac{1}{T_c} + \frac{1}{T_h}\right) \tag{11}$$

where n_c is the carrier density.

To calculate the rate of energy transfer from the hot electrons to the cooler holes, the expression derived by Asche and Sarbei [15] was used. This is a double integral and is derived by assuming that the electrons are described by Fermi–Dirac statistics and the holes can be described by a Maxwellian distribution. Alternatively, a triple integral can be derived that assumes that both the electrons and the holes are described by Fermi–Dirac statistics but this should not give any greater insight into the cooling of the plasma. As mentioned earlier it is acceptable to consider the screening of the e–h interaction by a simple static screening length that is calculated self-consistently. However, the screening efficiency of the electron will be greater than that of the hole due to the pronounced mass differences between the two particles. This was included in our simulation by assuming that only the electrons were capable of screening the interaction between the electrons and the holes [6].

The remaining two terms in equation (1) are that of radiative recombination [30] and Auger recombination. These effects are negligible on an ultrashort timescale but begin to play a minor role after a few picoseconds as they slow the carrier cooling down. We used a value of 2.6 ns for the lifetime of the carriers due to radiative recombination [9]. In GaAs carrier heating by Auger processes can usually be neglected due to the relatively small Auger coefficients. This is not the case in narrow-gap materials such as $In_{0.53}Ga_{0.47}As$. In undoped materials the heating rate is

$$\left(\frac{dE_c}{dt}\right)_{Aug} = C_A n_c^2 E_g \tag{12}$$

where E_g is the minimum energy gap between the conduction and valence band and C_A is the Auger coefficient. Here, we used a value of 7×10^{-29} cm^6 s^{-1} for C_A [9].

The rate of change of carrier density from the various processes that are occurring in the semiconductor may be written as

$$\left(\frac{\mathrm{d}n_c}{\mathrm{d}t}\right) = \left(\frac{\mathrm{d}n_c}{\mathrm{d}t}\right)_L + \left(\frac{\mathrm{d}n_c}{\mathrm{d}t}\right)_{rad} + \left(\frac{\mathrm{d}n_c}{\mathrm{d}t}\right)_{Aug} \tag{13}$$

where the various subscripts have the same meaning as in equation (1).

Starting from thermal equilibrium and calculating $(\mathrm{d}E_c/\mathrm{d}t)$ and $(\mathrm{d}n_c/\mathrm{d}t)$ at each time interval through and after the pump pulse E_c and n_c may be evaluated as a function of time. The remaining task is to find the solutions of the pair of simultaneous equations relating E_c and n_c to T_c and η_c (the quasi-Fermi energy) for each carrier distribution

$$\begin{aligned} &E_c - 3\left(\frac{2\pi m_c}{h^2}\right)^{3/2} (k_B T_c)^{5/2} F_{3/2}(\eta_c) = 0 \\ &n_c - 2\left(\frac{2\pi m_c k_B T_c}{h^2}\right)^{3/2} F_{1/2}(\eta_c) = 0 \end{aligned} \tag{14}$$

where $F_{1/2,3/2}(\eta_c)$ are the Fermi integrals. This explicitly incorporates the parabolic band approximation.

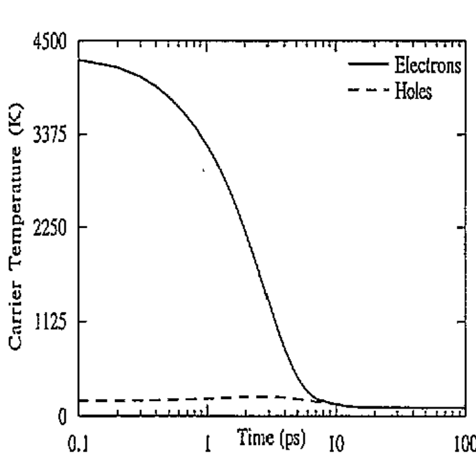

Figure 1. Electron and hole temperatures as a function of time in the single-valley model.

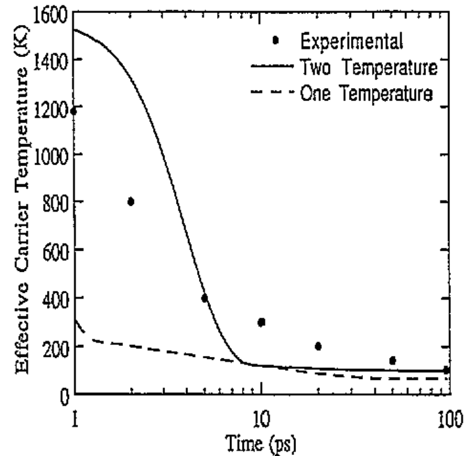

Figure 2. Effective carrier temperature in the single-valley model and in a model that assumes that both the electrons and holes are thermalized at the same carrier temperature.

In this way the effective temperatures and quasi-Fermi energies of the electrons and holes, created by a sub-picosecond laser pulse were calculated for the first 100 ps after excitation. Figure 1 shows a graph of the electron and hole temperatures obtained from the single-valley model. It can be seen that initially the electrons are at a far higher temperature than the holes and gradually come into equilibrium with them during the first

ten picoseconds. For times beyond ten picoseconds the electrons and holes can effectively be described by a single-carrier temperature.

It is not normally possible to measure experimentally the electron and hole temperatures simultaneously. Instead, an effective carrier temperature is usually extracted from the high-energy tail of the observed luminescence spectra [7]. This can be approximated by an exponential of the form

$$I(h\nu) \cong \exp\left(\frac{h\nu}{k_B T_{\rm eff}}\right) \tag{15}$$

where $T_{\rm eff}$ is the effective carrier temperature and is related to the electron and hole temperatures by the following expression:

$$\frac{m_e + m_h}{T_{\rm eff}} = \frac{m_h}{T_e} + \frac{m_e}{T_h}. \tag{16}$$

As shown in figure 2, a model that assumes both the electrons and holes are thermalized at the same carrier temperature at all times does not provide a very good fit to the experimental data. Previous authors [9, 11] have attributed the retarded cooling rate to be due exclusively to the hot phonon effect and introduced a reduction factor to account for this, but as our simulation shows, the hot phonon effect does not account for the reduced cooling rate in a single temperature model. A much larger effect is observed when the electrons and holes are allowed to thermalize at different temperatures. In this case the effective temperature of the carriers is greatly over-estimated for the first five picoseconds after excitation. The cooling rate then becomes too large and the effective carrier temperature drops below the measured value. It is clear that to describe accurately the plasma dynamics on a timescale of picoseconds rather than tens of picoseconds other effects need to be incorporated into the analytical model.

2.2. *Multiple-valley model*

The presence of higher valleys in the conduction band of $In_{0.53}Ga_{0.47}As$ can have a profound effect on the cooling of the photoexcited electrons providing that a sufficient proportion of the electrons in the Γ valley have enough excess energy above the Γ valley minimum to scatter to the higher valleys at the L and X points in the Brillouin zone. This rapid scattering acts as an effective cooling mechanism for the remaining electrons in the Γ valley on a subpicosecond timescale. The subsequent return of the L valley electrons to the Γ valley several picoseconds later acts as a source of heating to the Γ valley electrons so their net cooling rate is reduced. As the L valley minima lie approximately 0.55 eV above the Γ valley minima in $In_{0.53}Ga_{0.47}As$, a large proportion of the electrons initially lie above the threshold for transfer to the L valley. The presence of the higher X valleys are neglected in this calculation as their minima are expected to lie more than 1 eV above the Γ valley minimum [31].

The total number of electrons above the threshold is

$$n_{\rm thres} = 4\pi\left(\frac{2m_e k_B T_e}{h^2}\right)^{3/2} \int_{E_L/k_B T_e}^{\infty} \frac{\epsilon^{1/2}\,d\epsilon}{1+\exp(\epsilon-\eta_e)}. \tag{17}$$

The average energy per carrier above the threshold is

$$U_{\rm thres} = \frac{3(2\pi m_e/h^2)^{3/2}(k_B T_e)^{5/2}}{n_{\rm thres}} \int_{E_L/k_B T_e}^{\infty} \frac{\epsilon^{3/2}\,d\epsilon}{1+\exp(\epsilon-\eta_e)}. \tag{18}$$

E_L is the energy difference between the L valley minima and the Γ valley minimum. We chose to represent the transfer rates to and from the L valley by a simple time-independent scattering rate. Thus

$$\left(\frac{dn_e}{dt}\right)_{out} = -\frac{n_{thres}}{\tau_{\Gamma L}} \tag{19}$$

$$\left(\frac{dn_e}{dt}\right)_{in} = \frac{n_L}{\tau_{L\Gamma}} \tag{20}$$

where n_L is the number of electrons contained in the L valley and $\tau_{\Gamma L}$ and $\tau_{L\Gamma}$ are the scattering times to and from the L valley respectively. By adding (19) and (20) to the rate equation, (13), for the electrons with a similar expression being added to equation (1) relating to the energy transfer to and from the L valley the effects of intervalley scattering are incorporated into our analytical model.

3. Results

As previously shown, the model which neglected the higher valleys in the $In_{0.53}Ga_{0.47}As$ was incapable of providing a realistic description of the cooling of the photoexcited carriers. Figure 3 shows the behaviour of the effective carrier temperatures after excitation for the multiple-valley model for a range of scattering times to the L valley and a single return time of 9 ps, compared with experiment [22]. The effective carrier temperature is greatly reduced during the first five picoseconds compared with the single-valley model. This is the result of a much reduced electron temperature which is caused by the large number of high-energy electrons migrating to the L valley where they no longer contribute to the luminescence spectrum and hence no longer contribute to the measured carrier temperature. The hole temperature evolves almost identically in both models. It can clearly be seen that for $\tau_{\Gamma L} = 500 \pm 100$ fs, a very good fit is obtained to the experimental data. Scattering times lower than this lead to cooling rates during the first two picoseconds that are much higher than was experimentally observed. It appears that no work on the intervalley deformation potentials or on the intervalley scattering rates has been published for $In_{0.53}Ga_{0.47}As$ at 4 K. Results have been published on $In_{0.53}Ga_{0.47}As$ at room temperature though, by Kim *et al* [31]. They estimated a scattering time, $\tau_{\Gamma L}$, of 150 fs in $In_{0.53}Ga_{0.47}As$ by studying the cooling of hot carriers by subpicosecond Raman scattering. This was slightly larger than the value they obtained in GaAs at room temperature of around 100 fs due to the different band structure of the two compounds. The difference between the results of Kim *et al* [31] and our results is almost certainly due to the sample temperature at which the measurements were taken. A low sample temperature results in a low phonon mode occupancy at the zone edge which leads to a small intervalley scattering rate and hence a large scattering time. Recently, Zollner *et al* [32] have developed a semi-empirical model to calculate the intervalley deformation potentials in the rigid-ion approximation. Their theory predicts that $\tau_{\Gamma L}$ in InAs is greater than $\tau_{\Gamma L}$ in GaAs. It is reasonable to assume that this trend will be also observed in $In_xGa_{1-x}As$ as the ratio of In to Ga increases so $\tau_{\Gamma L}$ in the ternary compound $In_{0.53}Ga_{0.47}As$ should also be larger than $\tau_{\Gamma L}$ in GaAs. This assumption is in agreement with the results of Kim *et al* [31] that were mentioned above. Several conflicting reports have been published on GaAs at a lattice temperature of ~ 4 K in which the value of the scattering times from the Γ valley to the L valley were measured [33–35]. The values

obtained from these experiments for $\tau_{\Gamma L}$ ranged from 150 fs as measured by Fasol *et al* [33] to the value measured by Ulbrich *et al* [35] of 540 ± 120 fs. The scattering time that we obtained of 500 ± 100 fs is equal to or larger than the published results for GaAs which is what is expected assuming that $\tau_{\Gamma L}$ does increase from GaAs to $In_{0.53}Ga_{0.47}As$. Clearly, it will be extremely useful if the theoretical calculations of Zollner *et al* [32] can be extended to ternary alloys to allow a comparison to be made with our results.

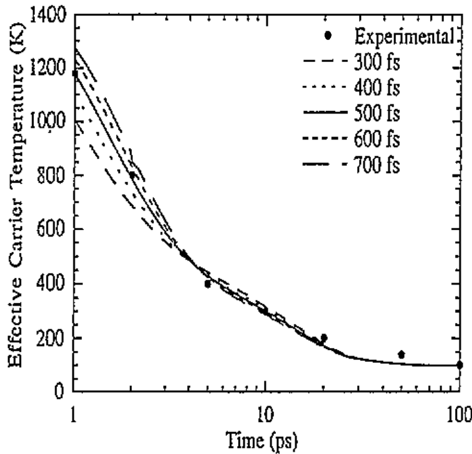

Figure 3. Effective carrier temperature as a function of time in the multiple-valley model. Experiment: solid circles. Theory: dashed and solid lines for several values of $\tau_{\Gamma L}$. $\tau_{L\Gamma} = 9.0$ ps in all cases.

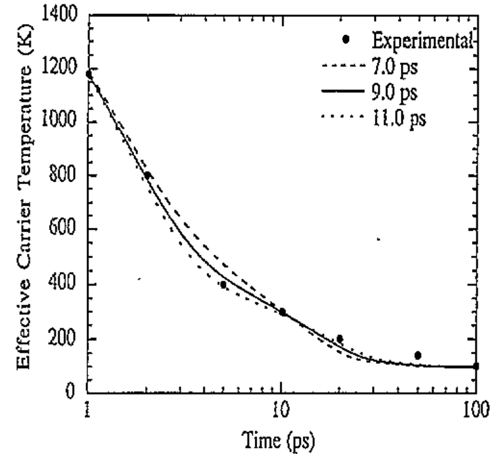

Figure 4. Effective carrier temperature as a function of time in the multiple-valley model. Experiment: solid circles. Theory: dashed and solid lines for three values of $\tau_{L\Gamma}$. $\tau_{\Gamma L} = 500$ fs in all cases.

In figure 4 we have plotted the temperature curves for the multiple-valley model for a scattering time, $\tau_{\Gamma L}$ of 500 fs and several return times. This shows the delayed heating effect as the high-energy electrons in the L valley slowly return to the Γ valley and redistribute their excess energy over the whole system. The model of Zollner *et al* [32] predicts that in GaAs at 4 K, the return time, $\tau_{L\Gamma}$, is 6.6 ± 0.5 ps. The best fit to our experimental data is obtained for $\tau_{L\Gamma} = 9 \pm 2$ ps which is again consistent with the expectation that the scattering time increases from GaAs to $In_{0.53}Ga_{0.47}As$. The main source of error in comparing the results of computer simulations with experimental values is the uncertainty in the carrier density that is created by the laser pulse. This can usually only be estimated to within a factor of ~ 2. By varying the carrier density within these bounds, the range in the effective temperature, for $\tau_{\Gamma L} = 500$ fs and $\tau_{L\Gamma} = 9$ ps at 1 ps was 1160–1220 K and at 5 ps was 430–470 K. This is the limiting factor in attempting to extract intervalley scattering rates from luminescence spectra.

Figure 5 is a graph of the electron density in the Γ and L valleys and the total electron density as a function of time. It can be seen that the electron density in the Γ valley initially increases as all the photoexcited electrons are created in the Γ valley. Over 30% of the electrons subsequently migrate to the L valley with the density reaching a peak of 7×10^{17} cm^{-3} after 1.5 ps. Beyond this time the energy of the Γ valley electrons drops too low for a sufficient number to be excited above the threshold level of 0.55 eV so the net effect is that the density of electrons in the L valley electrons decreases as these high-energy electrons begin to return to the Γ valley. The slope in the total carrier density curve that can

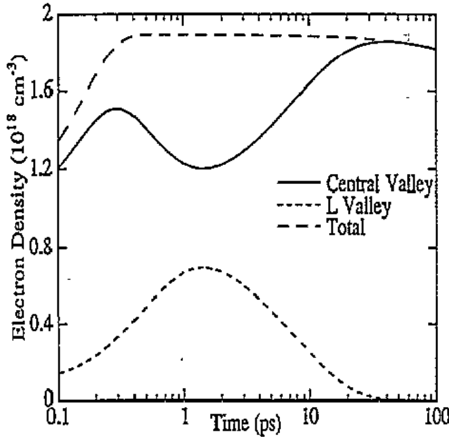

Figure 5. Evolution of the electron population in the central (Γ) valley and the L valley along with the total electron density curve.

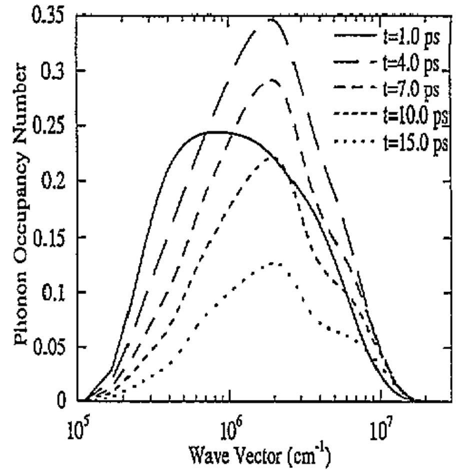

Figure 6. LO phonon occupation number versus phonon wave vector for five different times after photoexcitation.

be seen between 10 and 100 ps is due to radiative and Auger recombination. The maximum fraction of the electrons that transfer to the L valley is lower than in simulations by other authors [3, 18, 21]. This is due to two reasons; one is that the L valley minima lie further above the Γ valley minimum in $In_{0.53}Ga_{0.47}As$ than in GaAs so at our excitation energy fewer electrons lie above the threshold energy and secondly our simulation assumes that the $In_{0.53}Ga_{0.47}As$ is at 4 K so the scattering rate to the L valley is much lower than at room temperature.

Intervalley scattering to, and from, the X valley has been included in several calculations on ultrafast carrier relaxation by ensemble Monte Carlo techniques [6, 36]. In these calculations, the energy of the excitation pulse was greater than considered here, so a larger proportion of the hot electrons could, potentially, scatter to the X valley. It was found that the L valley population contained a significant number of electrons that made their way to the L valley via the X valley. The scattering times, $\tau_{\Gamma X}$ and $\tau_{X\Gamma}$, are smaller than $\tau_{\Gamma L}$ and $\tau_{L\Gamma}$. If a significant number of electrons can scatter to the X valley, it cools down the remaining electrons even more effectively during the first picosecond. Any error caused by our neglect of the X valley will manifest itself as an underestimation of $\tau_{\Gamma L}$ as this value will be a combination of both $\tau_{\Gamma L}$ and $\tau_{\Gamma X}$. The resulting transfer of electrons back from the X valley will be a complicated process as some electrons will return via the L valley. However, the effects of intervalley scattering to the X valley should be small in our simulation due to the small excitation energy of the electrons compared with the energy of the X valley minima.

In figure 6 the time evolution of the hot-LO-phonon population is plotted. The phonon population rises well above its equilibrium value within the first picosecond after excitation. After 1 ps the peak is at 1×10^6 cm^{-1}. This peak shifts as more phonons are emitted at a higher wavevector. The non-equilibrium phonon population reaches its maximum value after about 4 ps with a peak in the occupation number of $\sim$ 0.35 at a wavevector of 2×10^6 cm^{-1}. After 10 ps a shoulder is observable at 6×10^6 cm^{-1} due to emission of LO phonons by the holes. The effect of the non-equilibrium phonon population on the carrier temperature evolution is shown in figure 7. When the simulation was performed

neglecting both the possibility of a hot-phonon population and intervalley scattering a poor fit to the experimental; data was observed, the shape of the curve being similar to the two temperature model of figure 2. It was not possible to increase substantially the closeness of fit by varying the LO phonon relaxation time because increasing it had an adverse effect on the shape of the curve at short times while decreasing it had a negative effect at larger times. By including intervalley scattering but still neglecting hot phonons, a better fit to the experimental data was obtained but unless unrealistic values for $\tau_{L\Gamma}$ were used, the effective carrier temperature would still become smaller than was experimentally observed after about 10 picoseconds. It is in this regime that the retardation effect of the hot-phonon population becomes important.

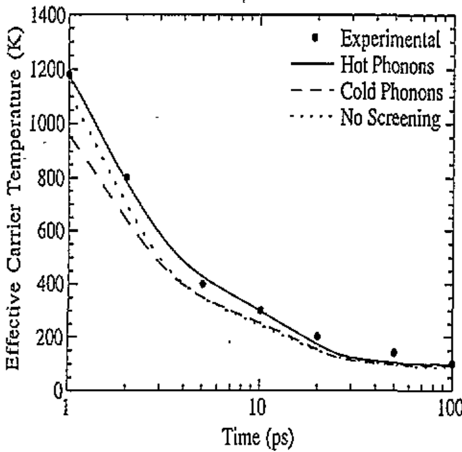

Figure 7. Effective carrier temperature in the multiple-valley model with and without the presence of hot phonons and also in a model which includes hot phonons but neglects screening of the c–ph interactions.

Also shown in figure 7 is a model which includes hot phonons but neglects screening of the c–ph interactions. It can be seen that there is a less than 15% difference between the effective carrier temperatures in the model which neglects c–ph screening and the one which includes it statically. Collet [24] recently considered whether a dynamical screening theory was required to treat accurately the c–ph interactions in GaAs. In his analysis the dynamical treatment of screening generally led to cooling rates that lay in between the rates for the no screening and the static screening model. The cooling curve for the dynamical model would then be intermediate between the curves given in figure 7. It is therefore valid to consider screening of all the e–ph and h–ph interactions via a simple static screening approximation rather than via a full dynamical treatment as any deviation from this should be less significant than the effects of other approximations in the model. Finally, it must be stressed that the carrier cooling rates are much less sensitive to the hot-phonon effect and to screening than they are to intervalley scattering because there is a trade-off between the strength of the screening and the amount of non-equilibrium phonon build-up. An increase in the screening strength will cause a *decrease* in the cooling rate but will also cause a reduction in the phonon build-up which will cause an *increase* in the cooling rate. Hence, screening and the hot-phonon effect tend to counteract each other [13].

4. Conclusions

We have presented a theoretical analysis of the cooling of highly photoexcited electrons and holes in intrinsic $In_{0.53}Ga_{0.47}As$. We modelled a 900 fs laster pulse which was used to create an initial plasma density of 1.9×10^{18} cm^{-3} at an excitation energy of 1.44 eV per carrier pair. The analytical model treated the electrons and holes as two different plasma subsystems and the phonons as a discrete set of phonon modes. It included the effects of the electron–hole interaction, carrier–phonon interaction, intervalley scattering to the L valley for the conduction band electrons and Auger and radiative recombination.

By comparing the model with recent experimental results it was shown that in order to model accurately the cooling of the carriers down to a timescale of one picosecond it is essential to include intervalley scattering as it acts as a very efficient form of energy storage for the electrons whereby there is a large initial fall in the electron energy followed by a subsequent retardation of the energy-loss rate. This enabled us to estimate scattering times, to and from, the L valley of 500 ± 100 fs and 9 ± 2 ps respectively. The limitations of this method as a way of obtaining more accurate values of the scattering times was noted due to the inherent uncertainty in the excited carrier density. The presence of a hot-phonon population caused by the rapid emission of LO phonons by the hot carriers was also seen to retard the cooling of the carriers.

The net result of this analysis is that we are now able to model the relaxation of hot electrons and holes in $In_{0.53}Ga_{0.47}As$ with good accuracy down to a timescale that has not previously been accessible [9–11] without having to resort to complicated Monte Carlo calculations.

Acknowledgment

This work was supported by the Science and Engineering Research Council.

References

[1] Elsaessar T, Shah J, Rota L and Lugli P 1991 *Phys. Rev. Lett.* **66** 1757
[2] Rota L, Lugli P, Elsaessar T and Shah J 1993 *Phys. Rev.* B **47** 4226
[3] Kim D S and Yu P Y 1991 *Phys. Rev.* B **43** 4158
[4] Kim D S, Jacob J M, Zhou J F, Song J J, Hou H, Tu C W and Morkoc H 1992 *Phys. Rev.* B **45** 13973
[5] Zhou X Q, Leo K and Kurz H 1992 *Phys. Rev.* B **45** 3886
[6] Hohenester U, Supancic P, Kocevar P, Zhou X Q, Kutt W and Kurz H 1993 *Phys. Rev.* B **47** 13233
[7] Collet J H, Ruhle W W, Pugnet M, Leo K and Million A 1989 *Phys. Rev.* B **40** 12296
[8] Bradley C W W, Taylor R A and Ryan J F 1989 *Solid-State Electron.* **32** 1173
[9] Lobentanzer H, Stolz W, Nagle J and Ploog K 1989 *Phys. Rev.* B **39** 5234
[10] Westland D J, Ryan J F, Scott M D, Davies J I and Riffat J F 1988 *Solid-State Electron.* **31** 431
[11] Kash K and Shah J 1984 *Appl. Phys. Lett.* **45** 401
[12] Pugnet M, Collet J and Comet A 1981 *Solid State Commun.* **38** 531
[13] Potz W and Kocevar P 1983 *Phys. Rev.* B **28** 7040
[14] Potz W 1987 *Phys. Rev.* B **36** 5016
[15] Asche M and Sarbei O G 1984 *Phys. Status Solidi* b **126** 607
[16] Asche M and Sarbei O G 1987 *Phys. Status Solidi* b **141** 487
[17] Osman M A and Ferry D K 1987 *Phys. Rev.* B **36** 6018
[18] Lugli P, Bordone P, Reggiani L, Reiger M, Kocevar P and Goodnick S M 1989 *Phys. Rev.* B **39** 7852
[19] Joshi R P, Grondin R O and Ferry D K 1990 *Phys. Rev.* B **42** 5685
[20] Shah J, Deveaud B, Damen T C, Tsang W T, Gossard A C and Lugli P 1987 *Phys. Rev. Lett.* **59** 2222
[21] Gong T, Fauchet P M, Young J F and Kelly P J 1991 *Phys. Rev.* B **44** 6542

[22] Gregory A, Usher S, Majumder F A and Phillips R T 1993 *Solid State Commun.* **87** 605
Gregory A, Phillips R T and Majumder F 1991 *Proc. SPIE* **1362** 268
[23] Osman M A, Cahay M and Grubin H L 1989 *Solid-State Electron.* **32** 1911
[24] Collet J H 1989 *Phys. Rev.* B **39** 7659
[25] von der Linde D, Kuhl J and Klingenburg H 1980 *Phys. Rev. Lett.* **44** 1505
[26] Kash J A, Tsang J C and Huam J M 1985 *Phys. Rev. Lett.* **54** 2151
[27] The chapter by J Shah in
Devreese J T and Peeters F M (ed) 1987 *The Physics of a Two Dimensional Electron Gas, Proc. NATO Advanced Study Inst. (Oostduinkerke, Belgium, 1986)* (New York: Plenum)
provides a complete derivation of this equation in a similar form.
[28] Kocevar P 1972 *J. Phys. C: Solid State Phys.* **5** 3349
[29] Wiley J D 1971 *Phys. Rev.* B **4** 2485
[30] Bimberg D and Mycielski J 1985 *Phys. Rev.* B **31** 5490
[31] Kim D S and Yu P Y 1990 *Appl. Phys. Lett.* **56** 1570
[32] Zollner S, Gopolan S and Cardona M 1992 *Semicond. Sci. Technol.* **7** B137
[33] Fasol G, Hackenburg W, Hughes H P, Ploog K, Bauser E and Kano H 1990 *Phys. Rev.* B **41** 1461
[34] Mirlin D N, Karlik I Ja, Nikitin L P, Reshina I I and Sapega V F 1981 *Solid State Commun.* **37** 757
[35] Ulbrich R F, Kash J A, Tsang J C 1989 *Phys. Rev. Lett.* **62** 949
Alekseev M A and Mirlin D N 1990 *Phys. Rev. Lett.* **65** 274
Kash J A, Tsang J C and Ulbrich R G 1990 *Phys. Rev. Lett.* **65** 275
[36] Kann M J, Kriman A M and Ferry D K 1990 *Phys. Rev.* B **41** 12659
[37] The values in table 1 were obtained from
Pearsall T P (ed) 1982 *GaInAsP Alloy Semiconductors* (New York: Wiley)